Tetrahedron: *Asymmetry* 20 (2009) 1365–1368

Contents lists available at ScienceDirect

Tetrahedron: *Asymmetry*

journal homepage: www.elsevier.com/locate/tetasy

The mechanism of enantioselective control of an organocatalyst with central and axial chiral elements

Dezhan Chen *, Nan Lu, Guiqiu Zhang, Shizhen Mi

College of Chemistry, Chemical Engineering and Materials Science, Shandong Normal University, Jinan 250014, PR China

ARTICLE INFO

Article history:
Received 21 April 2009
Accepted 19 May 2009
Available online 27 June 2009

ABSTRACT

The mechanism of the enantioselective control of an organocatalyst with central and axial chiral elements in the Michael addition of 2,4-pentandione to a nitroalkene is investigated using density functional theory (DFT) calculations. Two enantioselective channels are characterized in detail. Enantioselectivity is determined in the C–C bond coupling and the proton transfer is identified as the energetic bottleneck. Generally, the level of enantioselectivity of the catalysts depends on the geometrical match or mismatch of two asymmetric elements. The 'closed' geometry of a catalyst makes the cooperation of two chiralities possible, so that the central and axial chiralities work together to enhance the enantioselective control. The 'open' structure of catalyst makes cooperation of the two asymmetric elements impossible, so that its enantioselectivity dominated only by one type of chirality is decreased.

1. Introduction

The Michael addition of a carbon nucleophile to a nitro olefin provides rapid access to chiral nitroalkane, a class of building block and important intermediate in organic synthesis.[1] Over the past decade, a catalytic asymmetric version of the process has been achieved, albeit requiring a metal catalyst or strict reaction conditions.[2–4] Recently, significant advances were made by using an organocatalyst[5,6] to reduce the expense and possible contamination by metals.[7] However, the number of successful organocatalysts involving two chiral elements is small.[8]

In the past, organocatalysts only containing central chirality have been widely used for various asymmetric transformations.[9–12] Other types of axially chiral organocatalysts have significant reactivity and enantioselectivity, such as a C_2 symmetric chiral ketone,[13] iridium QUINAP complex,[14] binaphthyl-derived Brønsted acid,[15,16] and bis(thio)urea derived from H_8-BINAM.[17] Research on the cooperative effect of multi-component asymmetric elements in one molecule has received considerable attention because correct assembly of central and axial chiralities could facilitate its tunability and achieve high enantioselectivity.[18] Recently, two novel organocatalysts incorporating central and axial chiralities have been synthesized for the Michael addition.[8] (*R*,*R*,*R*)-catalyst **cat 1** gave (*S*)-adduct with 93% ee, whereas (*R*,*S*,*S*)-catalyst **cat 2** afforded the (*R*)-adduct with a lower enantioselectivity (78% ee).

Hence there are two questions about this reaction. What is the reason for the opposite stereochemical preference of two catalysts? and what is the reason for different levels of enantioselectivity that are matched and mismatched in experiment? We have initiated a theoretical investigation of the Michael addition of 2,4-pentandione to nitroalkene using two organocatalysts (Scheme 1) to answer these two questions.

2. Computational details

All calculations were performed with GAUSSIAN 03 software package[19] under a DFT framework. All stationary points on the potential energy surface (PES) were optimized using the hybrid functional B3LYP[20] and 6-31G(d) basis set without any symmetric restriction under solvent-free conditions while their nature (minima or first-order saddle-points) was characterized by performing vibrational frequency calculations. The intrinsic reaction coordinate (IRC) paths were traced in order to verify two desired minima connected by the transition states (TSs). To obtain accurate energetics, additional single point energy calculations were performed at a B3LYP/6-311++G** level. For all energies cited, the zero-point energy (ZPE) corrections were included.

3. Results and discussion

In the reaction, organocatalysts are modeled by their truncated form involving necessary chiral elements. Reactants and catalysts denoted as **e**, **nu**, **cat 1**, and **cat 2** are first optimized (Fig. 1). **Nu** can tautomerize to enol and keto forms in equilibrium. With an intramolecular H bond of 1.63 Å, the cyclic enol form of **nu** is more stable and the nucleophilic character of the reacting carbon center is enhanced when compared with the keto form. Hence we consider only its enol form in the reaction. To achieve initial activation, **nu** is deprotonated by the tertiary amine N of the catalysts to give

* Corresponding author.
E-mail address: dchen@sdnu.edu.cn (D. Chen).

0957-4166/$ - see front matter © 2009 Published by Elsevier Ltd.
doi:10.1016/j.tetasy.2009.05.027

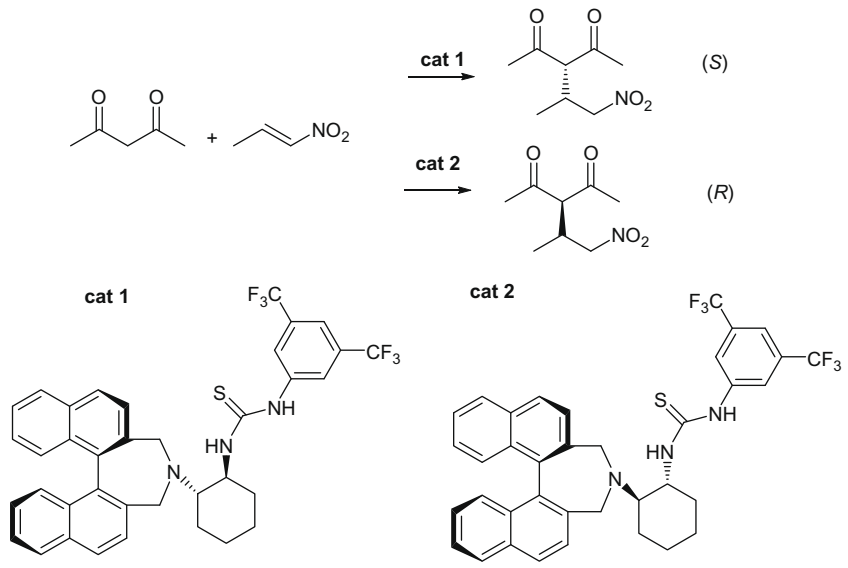

Scheme 1. Enantioselective Michael addition of 2,4-pentandione to nitroalkene promoted by two catalysts.

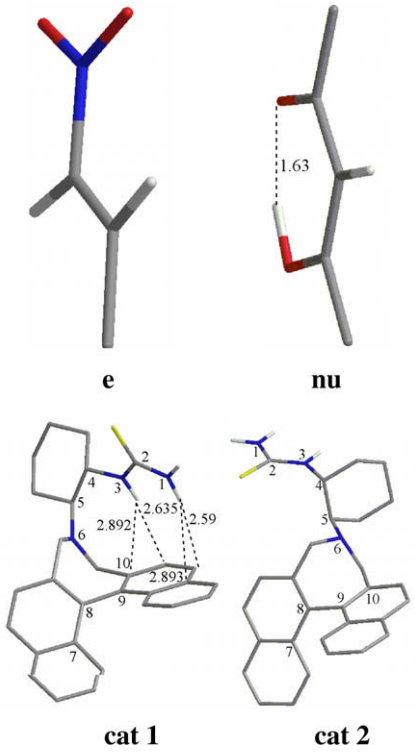

Figure 1. Optimized structure of reactants and catalysts. (The hydrogen atoms on the rings are omitted for clarity.)

reactive enolates **1-1** and **2-1**, where the first number denotes the catalysts and the second is related to steps. (The same is as follows.)

The Michael reaction between **e** and **1-1** (**2-1**) can take place via two steps: C–C bond coupling and proton transfer. The TSs are denoted as **TS-1s1**, **TS-1s2**, **TS-1r1**, and **TS-1r2** with **cat 1** and **TS-2s1**, **TS-2s2**, **TS-2r1**, and **TS-2r2** with **cat 2**, respectively (Fig. 2).

3.1. Structural characteristic of main TSs

With the geometry of pre-TSs and the resulting intermediates optimized in hand, we studied TSs via a QST3 method. TS optimizations were carried out using the resultant geometry of the previous step as input data. By performing vibrational frequency calculations, we believed that the reality of TSs was verified through one imaginary frequency.

For the reaction with **cat 1**, the lengths of the forming C–C bond in **TS-1s1** and **TS-1r1** are 2.088 and 2.259 Å, respectively. The smaller imaginary vibrational frequency of **TS-1r1** (235i cm^{-1}) compared to **TS-1s1** (303i cm^{-1}) indicates that **e** and **nu** are loosely bound in **TS-1r1**. The compact assembly of **TS-1s1** makes it more stable than **TS-1r1**. For proton transfer, the H bonds between thiourea and nitryl O of **TS-1s2** (1.803, 2.295 Å) are shorter than those of **TS-1r2** (1.873, 2.970 Å). The weaker interaction between **e** and **cat 2** in **TS-1r2** makes it less stable than **TS-1s2**, which is in line with the smaller imaginary frequency of **TS-1r2** (1213i cm^{-1}) than that of **TS-1s2** (1325i cm^{-1}).

In the case of **cat 2**, the H-bonded network of **TS-2r1** (1.708, 1.854, 2.155, and 2.591 Å) is slightly more compact than that of **TS-2s1** (1.731, 1.866, 2.183, and 2.488 Å). This might contribute to the imaginary vibrational frequency of **TS-2s1** (280i cm^{-1}) a little smaller than that of **TS-2r1** (284i cm^{-1}). In the proton transfer step, **TS-2s2** possesses H bonds (2.255, 2.758 Å) weaker than that of **TS-2r2** (1.937, 2.008 Å). Due to the smaller imaginary frequency of **TS-2s2** (1061i cm^{-1}) than that of **TS-2r2** (1272i cm^{-1}), **TS-2r2** is consequently more stable than **TS-2s2**. The above analysis provides the primary indication of the opposite stereochemical preference of two catalysts.

3.2. Energetic profiles

Figures 3 and 4 depict the calculated energetic profiles for the reaction. In the case of **cat 1**, complexes **1-2s** and **1-2r** between **1-1** and **e** were located as initial intermediates of the two enantioselective channels. The C–C bond coupling takes place via **TS-1s1** with a barrier of 10.43 kcal mol^{-1} from **1-2s** yielding a stable intermediate **1-3s**. This step is exothermic by 6.58 kcal mol^{-1}. While in (*R*)-channel, this step is required to be endothermic by 0.82 kcal mol^{-1}, with a barrier 1.56 kcal mol^{-1} higher than that of (*S*)-channel. This result indicates that the (*S*)-channel is more favorable both thermodynamically and kinetically than (*R*)-channel. (*S*)-adduct is preferential with **cat 1** and is determined in this step. The barriers of proton transfer in the two channels are 21.78 (*S*) and 25.08 (*R*) kcal mol^{-1}, both higher than those of C–C bond

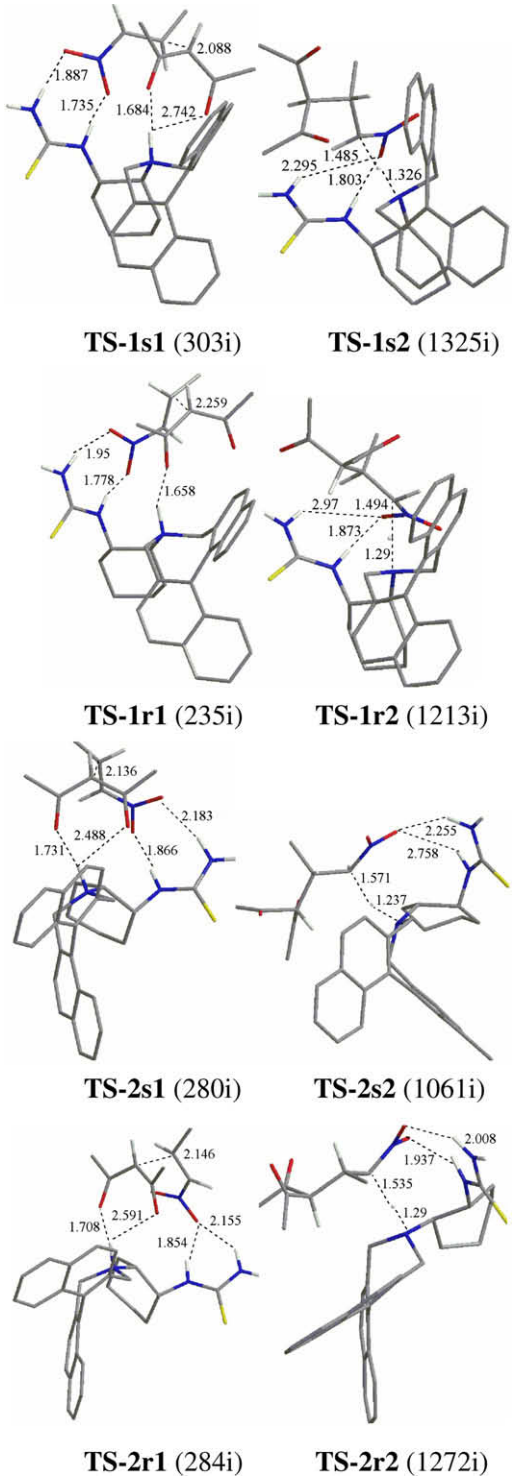

Figure 2. Optimized structure and selected geometric parameters of the TSs located along two channels with two catalysts. (The hydrogen atoms on the rings are omitted for clarity.)

coupling. This suggests that the rate-determining step of this Michael reaction is the proton transfer. Moreover, the barrier of the (*S*)-channel is 3.3 kcal mol^{-1} lower than that of the (*R*)-channel, which further confirms the preference of the (*S*)-adduct with **cat 1**.

For **cat 2**, the C–C bond coupling of the (*S*)-channel occurs via **TS-2s1** with a barrier of 14.66 kcal mol^{-1}, higher than that of (*R*)-channel (11.07 kcal mol^{-1}). The proton transfer of the (*S*)-channel occurs via **TS-2s2** with a barrier of 17.59 kcal mol^{-1}, also higher than that of the (*R*)-channel (15.66 kcal mol^{-1}). This demonstrates

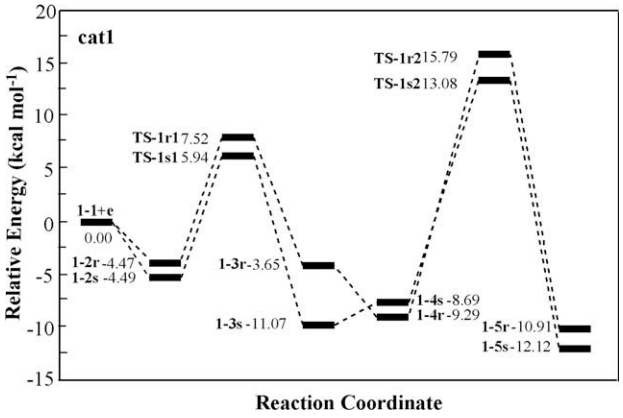

Figure 3. Calculated energetic profiles along the reaction coordinate with **cat 1**.

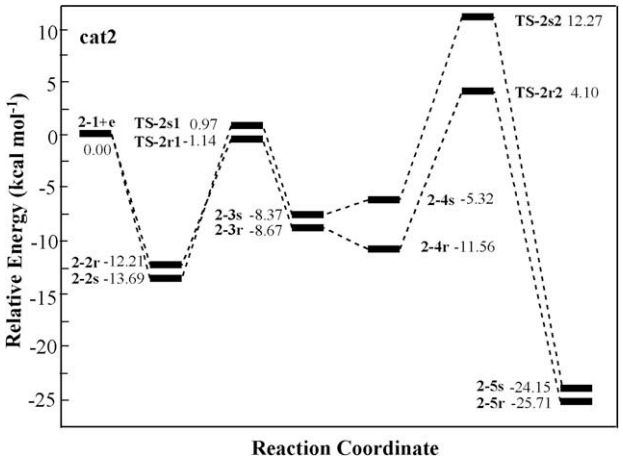

Figure 4. Calculated energetic profiles along the reaction coordinate with **cat 2**.

that in the case of **cat 2**, the (*R*)-adduct is preferable and the rate-determining step is still the proton transfer. It should be noted that the first step in the preferred (*R*)-channel of **cat 2** is endothermic by 3.54 kcal mol^{-1}. Comparing the (*S*)-channel with **cat 1** (−6.58 kcal mol^{-1}), it can be seen that the enantioselectivity of **cat 1** is higher than that of **cat 2**. This is in accordance with the 93% ee (*S*) for **cat 1** and 78% ee (*R*) for **cat 2** experimentally.[8]

3.3. Essence of enantioselectivity

Since the axial chiral element in (*R*,*R*,*R*)-**cat 1** and (*R*,*S*,*S*)-**cat 2** is the same, we expect that it is the central chirality of the catalyst that determines the absolute configuration of the product. As can be seen from Table 1, the changes of three dihedral angles from isolated **cat 1** to **TS-1s1** are smaller than those to **TS-1r1**. Apparently, (*S*)-channel is readily accessible with **cat 1**. This tendency is opposite in the case of **cat 2**. The changes of three dihedral angles

Table 1
The selected dihedral angles (°) of the optimized structure of **cat 1**, **cat 2**, and TSs (changes relative to isolated catalyst in parentheses)

	D1 N1–C2–N3–C4	D2 N3–C4–C5–N6	D3 C7–C8–C9–C10
cat 1	179.09	53.30	121.50
TS-1s1	−173.87(7.04°)	54.12(0.82°)	124.74(3.24°)
TS-1r1	−166.12(14.79°)	51.64(2.48°)	125.52(4.02°)
cat 2	−177.70	−164.43	124.12
TS-2s1	18.95(21.25°)	19.69(35.26°)	123.81(0.31°)
TS-2r1	11.79(14.09°)	18.05(33.62°)	124.04(0.08°)

Table 2
Activation thermodynamic properties[a] and energy barriers[b] calculated for the reaction catalyzed by **cat 1** and **cat 2**

	$\Delta H^{\neq}$ (kcal/mol)	$\Delta G^{\neq}$ (kcal/mol)	$\Delta S^{\neq}$ (J/mol)	Ea (kcal/mol)
TS-1s1	9.58	13.25	−51.53	10.43
TS-1s2	25.68	26.33	**−9.13**	**21.78**
TS-1r1	11.26	15.79	−63.60	11.99
TS-1r2	29.10	28.76	**4.77**	**25.08**
TS-2s1	14.30	18.59	−60.23	14.66
TS-2s2	19.18	19.69	**−7.16**	**17.59**
TS-2r1	11.79	18.05	−87.89	11.08
TS-2r2	17.32	18.39	**−15.03**	**15.66**

Bold entities are data applied to calculate ee values with Eqs. 1 and 2.
[a] Geometry optimization.
[b] Single point energy calculations at B3LYP/6-311++G(d,p) level.

from isolated **cat 2** to **TS-2s1** are bigger than that to **TS-2r1**. It is evident that the (*R*)-channel is favored by **cat 2**. Thus the origin of the opposite stereochemical preference of two catalysts is clearly understood.

From a chiral element point of view, dihedral angles D1 and D2 denote central chirality. D3 denotes the axial chirality. The change of the dihedral angle denotes the function of corresponding chirality in enantioselective control. From isolated **cat 1** to TSs, the changes of D1 and D2 are comparable to that of D3, which indicates that two chiral elements in **cat 1** have almost the same function in enantioselective control. On the other hand, the 'closed' geometry of **cat 1** (Fig. 1) resulting from the strong covalent interaction between the thiourea unit and carbons on one part of binaphthyl makes the cooperation of two chiralities possible so that the enantioselectivity is increased. Accordingly, this strong interaction of chiral elements enhances the stereochemical control and induces the higher enantioselectivity of **cat 1** (93% ee) than hydroxyl-thiourea (71% ee) only containing central chirality that we had previously studied.[21]

However, in the case of **cat 2**, changes of D1 and D2 are much larger than that of D3. Compared with **cat 1**, axial chirality of **cat 2** has almost no function in enantioselective control. This is because the 'open' structure of **cat 2** with thiourea and binaphthyl stretching in opposite directions makes the cooperation of the two asymmetric elements impossible so that its enantioselectivity is decreased (78% ee). These results demonstrate that the central and axial chiralities work together to enhance the enantioselective control for **cat 1**. In the case of **cat 2**, the enantioselectivity is dominated only by the central chirality. Generally, the level of enantioselectivity of the catalysts depends on geometrical match or mismatch of the two asymmetric elements.

Three activation thermodynamic properties and energy barriers of the two steps for the reaction were calculated (Table 2). Based on transition state theory and the kinetic interpretation of the Arrhenius equation,[22] the ee values were also calculated using Eqs. 1 and 2 with data from the rate-determining step. The results, 96.0% (*S*) of **cat 1** and 81.9% (*R*) of **cat 2**, are both overestimated compared with the experimental data, 93% (*S*) and 78% (*R*). Nevertheless, they do provide the correct indication of the stereochemical preference of the two catalysts and display the superiority of **cat 1** to **cat 2** in enantioselective control.

$$k = A\exp\left(\frac{-Ea}{RT}\right) = \frac{k_B T}{h} e^{n} (C^{\Theta})^{1-n} \exp\left(\frac{\Delta S^{\neq}}{R}\right) \exp\left(\frac{-Ea}{RT}\right) = Z_0 \exp\left(\frac{\Delta S^{\neq}}{R}\right) \exp\left(\frac{-Ea}{RT}\right) \quad (1)$$

$$\mathrm{ee} = \frac{[S]-[R]}{[S]+[R]} \cdot 100\% = \frac{|\,k_R - k_S\,|}{k_R + k_S} \cdot 100\% \quad (2)$$

4. Conclusion

Our DFT calculations provide a key basis for interpreting the essence of the enantioselectivity of organocatalyst with central and axial chiral elements in Michael addition. The calculated barrier of two enantioselective channels and the ee values provide the correct indication of the opposite stereochemical preference between two catalysts. Generally, the level of enantioselectivity of catalysts with central and axial chiral elements depends on a geometrical match or mismatch of the two asymmetric elements. If the catalyst has a 'closed' geometry, the central chirality and axial chirality work together to enhance the enantioselective control. If the catalyst has an 'open' structure, the cooperation of two asymmetric elements is impossible so that its enantioselectivity dominated only by one type of chirality is decreased. The present results will play an important role in the synthesis of geometrically matched organocatalysts.

Acknowledgments

This work was supported by National Basic Research Program of China (973 Program, 2007CB936000) and National Natural Science Foundations of China (No. 20675049).

References

1. Ballini, R.; Petrini, M. *Tetrahedron* **2004**, *60*, 1017–1047.
2. Evans, D. A.; Seidel, D. *J. Am. Chem. Soc.* **2005**, *127*, 9958–9959.
3. Watanabe, M.; Ikagawa, A.; Wang, H.; Murata, K.; Ikariya, T. *J. Am. Chem. Soc.* **2004**, *126*, 11148–11149.
4. Duursma, A.; Minnaard, A. J.; Feringa, B. L. *J. Am. Chem. Soc.* **2003**, *125*, 3700–3701.
5. Xiong, Y.; Wen, Y.; Wang, F.; Gao, B.; Liu, X.; Huang, X.; Feng, X. *Adv. Synth. Catal.* **2007**, *349*, 2156–2166.
6. Wei, S.; Yalalov, D. A.; Tsogoeva, S. B.; Schmatz, S. *Catal. Today* **2007**, *121*, 151–157.
7. Kobayashi, S.; Manabe, K. *Acc. Chem. Res.* **2002**, *35*, 209–217.
8. Peng, F. Z.; Shao, Z. H.; Fan, B. M.; Song, H.; Li, G. P.; Zhang, H. B. *J. Org. Chem.* **2008**, *73*, 5202–5205.
9. Taylor, M. S.; Jacobsen, E. N. *Angew. Chem., Int. Ed.* **2006**, *45*, 1520–1543.
10. Zu, L.; Wang, J.; Li, H.; Xie, H.; Jiang, W.; Wang, W. *J. Am. Chem. Soc.* **2007**, *129*, 1036–1037.
11. Amere, M.; Lasne, M. C.; Rouden, J. *Org. Lett.* **2007**, *9*, 2621–2624.
12. Cao, C.; Ye, M.; Sun, X.; Tang, Y. *Org. Lett.* **2006**, *8*, 2901–2904.
13. Dan, Y.; Yip, Y. C.; Tang, M. W.; Wong, M. K.; Zheng, J. H.; Cheung, K. K. *J. Am. Chem. Soc.* **1996**, *118*, 491–492.
14. Li, X. S.; Kong, L. C.; Gao, Y. G.; Wang, X. X. *Tetrahedron Lett.* **2007**, *48*, 3915–3917.
15. McDougal, N. T.; Schaus, S. E. *J. Am. Chem. Soc.* **2003**, *125*, 12094–12095.
16. Hashimoto, T.; Hirose, M.; Maruoka, K. *J. Am. Chem. Soc.* **2008**, *130*, 7556–7557.
17. Shi, M.; Liu, X. G. *Org. Lett.* **2008**, *10*, 1043–1046.
18. Wang, Y.; Li, X.; Ding, K. L. *Tetrahedron Lett.* **2002**, *43*, 159–161.
19. Frisch, M. J.; Trucks, G. W.; Schlegel, H. B.; Scuseria, G. E.; Robb, M. A.; Cheeseman, J. R.; Montgomery, J. A., Jr.; Vreven, T.; Kudin, K. N.; Burant, J. C.; Millam, J. M.; Iyengar, S. S.; Tomasi, J.; Barone, V.; Mennucci, B.; Cossi, M.; Scalmani, G.; Rega, N.; Petersson, G. A.; Nakatsuji, H.; Hada, M.; Ehara, M.; Toyota, K.; Fukuda, R.; Hasegawa, J.; Ishida, M.; Nakajima, T.; Honda, Y.; Kitao, O.; Nakai, H.; Klene, M.; Li, X.; Knox, J. E.; Hratchian, H. P.; Cross, J. B.; Adamo, C.; Jaramillo, J.; Gomperts, R.; Stratmann, R. E.; Yazyev, O.; Austin, A. J.; Cammi, R.; Pomelli, C.; Ochterski, J. W.; Ayala, P. Y.; Morokuma, K.; Voth, G. A.; Salvador, P.; Cioslowski, J.; Stefanov, B. B.; Liu, G.; Liashenko, A.; Piskorz, P.; Komaromi, I.; Martin, R. L.; Fox, D. J.; Keith, T.; Al-Laham, M. A.; Peng, C. Y.; Nanayakkara, A.; Challacombe, M.; Gill, P. M. W.; Johnson, B.; Chen, W.; Wong, M. W.; Gonzalez, C.; Pople, J. A. GAUSSIAN 03, Revision A. 1; Gaussian: Pittsburgh, PA, 2003.
20. Becke, A. D. *J. Chem. Phys.* **1993**, *98*, 1372–1377.
21. Chen, D. Z.; Lu, N. *Int. J. Quant. Chem.* **2008**, under review.
22. Truhlar, D. G.; Garrett, B. C.; Klippenstein, S. J. *J. Phys. Chem.* **1996**, *100*, 12771–12800.